Specular Reflectance Measurements of Dielectric Plates in Millimeter Frequency Range

Jin-Seob Kang[1,*] · Jeong-Hwan Kim[1] · Kwang Yong Kang[2] · Dae Hwan Yoon[3] · Sung Won Park[3]

Abstract

This paper describes specular reflectance measurements of dielectric plates in three waveguide frequency bands: D-band (110–170 GHz), G-band (140–220 GHz), and J-band (220–325 GHz). The transmit (Tx) part of the proposed specular reflectance measurement system is stationary, while the receive (Rx) part and the material under test (MUT) holder are concentric-rotating with a 2:1 speed ratio for specular reflectance measurements. In specular reflectance measurements, the first step measures the specular reflection coefficients of an MUT and a metal plate on the MUT holder located at the center of the Tx and Rx parts, and the second step calculates the specular reflectance defined by the specular reflection power (i.e., intensity) of the MUT normalized to that of the metal plate. Multiple reflection effects between the Tx and Rx antennas and the MUT on the measured specular reflectance are minimized by averaging out the multiple specular reflectances measured with changing the separation distance between the two antennas by $\lambda/8$ intervals. Measurement results of the perpendicular-polarized specular reflectance of commonly used dielectric plates are verified by comparing those with the analytic results and show that the results measured over the overlapped frequency range of the D-/G-bands and at the boundary frequency of the G-/J-bands agree well with the results for the other band, respectively.

Key Words: Dielectric Plate, Material Measurements, Millimeter-Wave, Multiple Reflections, Specular Reflectance.

I. INTRODUCTION

Recently, uses and applications of electromagnetic (EM) materials, devices, and systems have been becoming more popular in the fields of both the natural sciences, such as physics, chemistry, biology, earth science, and astronomy, and the application sciences, such as telecommunications, military, defense, security, transportation, and medicine. Their bandwidths have been broadening and operating frequency bands have been moving to the submillimeter frequency range. Measurements of the electrical properties of EM materials have gained considerable importance, particularly in the millimeter and submillimeter frequency ranges, as material parameters are fundamental parameters in the natural and application sciences fields [1, 2].

Various methods have been developed in millimeter and submillimeter frequency ranges to measure material properties (usually complex permittivity and permeability), e.g., the open resonator [3, 4], free space [5–10], and reflection ellipsometry methods [11–13]. The open resonator method provides accurate material properties at discrete resonance frequencies. The free space method is based on the quasi-optic approach where the material under test (MUT) is coupled to transmit (Tx) and

receive (Rx) antennas that are connected to the test ports of an *S*-parameter measuring instrument through two focused Gaussian beams generated by spot-focused horn lens antennas [5, 6], corrugated horn antennas with mirrors [7–9], and planar focusing arrays [10]. The reflection ellipsometry method is a well-established method for material characterization in optics and has been recently adapted to millimeter frequencies to determine material properties from the change of the polarization state of the wave reflected by an MUT that is illuminated by the linear-polarized wave radiated by a Tx antenna.

Recently, high speed and high data-rate communications have attracted considerable attention. The IEEE 802.15 THz Interest Group (IEEE 802.15 IGthz) has been performing a channel characteristics study for future millimeter and submillimeter indoor wireless communications in the frequency ranges of 75–110 GHz and 270–320 GHz [14].

As one of the important electrical parameters of indoor interior materials, specular reflectance, which is defined as the specular reflection power (i.e., intensity) of a dielectric plate normalized to that of a metal plate, is a prerequisite to the analysis of the channel characteristics for new millimeter and submillimeter indoor wireless communications. Specular reflection, as described by the law of reflection, is the direction of the incident wave and the direction of the reflected wave that make the same angle with respect to the surface normal of an MUT; thus, the angle of incidence is equal to that of reflection ($\theta_i = \theta_r$), as shown in Fig. 1.

This paper describes the specular reflectance measurements of dielectric plates in the 110–325 GHz frequency range. Preliminary results were given in [15], and in this paper, the work is extended by a detailed measurement procedure describing the calibration of a proposed specular reflectance measurement system, comparison of measurement results with those calculated from the analytic solution, and an in-depth analysis of measurement results. Section II briefly describes the analytic solution of the perpendicular-polarized specular reflection of a single-layer homogeneous isotropic dielectric plate, which is necessary

to verify measured specular reflectances of MUTs. Sections III and IV describe a proposed specular reflectance measurement system and its measurement procedure, respectively. Section V shows measurement results of the perpendicular-polarized specular reflectance of commonly used dielectric plates and verifies the measured results. Finally, Section VI summarizes this work.

II. Specular Reflection of a Homogeneous Dielectric Plate

When a perpendicular-polarized plane wave is incident upon a single-layer homogeneous isotropic dielectric plate of thickness t, as shown in Fig. 1(a), the specular reflection coefficient of the dielectric plate is given by [11]

$$R_{\text{Specular}} = \frac{E_r(\theta_r=\theta_i)}{E_i(\theta_i)} = \frac{1-\exp(-2j\beta)}{1-R_{\text{Interface}}^2\exp(-2j\beta)} R_{\text{Interface}}, \quad (1)$$

where $\beta = k_o t\sqrt{\varepsilon_r - \sin^2\theta_i}$ is the propagation factor through the dielectric plate, $k_o = 2\pi/\lambda_o$ is the free-space wavenumber, λ_o is the free-space wavelength, $\varepsilon_r = \varepsilon_r' - j\varepsilon_r''$ is the complex relative permittivity of the dielectric plate, θ_i and θ_r, respectively, are the incident and reflected angles, and $R_{\text{Interface}}$ is the perpendicular-polarized reflection coefficient at the air-dielectric interface, which is given by

$$R_{\text{Interface}} = \frac{\cos\theta_i - \sqrt{\varepsilon_r - \sin^2\theta_i}}{\cos\theta_i + \sqrt{\varepsilon_r - \sin^2\theta_i}}. \quad (2)$$

III. Specular Reflectance Measurement System

A specular reflectance measurement system is designed to measure both the magnitude and phase of the specular reflection of dielectric plates in the incident angle range of 30°–70° from the surface normal of an MUT in the frequency range for 110–325 GHz. The specular reflectance measurement system consists of an *S*-parameter measuring instrument and a specular reflectance measurement apparatus, as shown in Fig. 2.

The *S*-parameter measuring instrument consists of a 67 GHz vector network analyzer used as the main frame and three frequency extenders which are operating at three waveguide frequency bands, respectively: D-band (110–170 GHz, WR-6.5), G-band (140–220 GHz, WR-5.1), and J-band (220–325 GHz, WR-3.4). The vector network analyzer and frequency extender are connected to each other via phase stable RF and LO cables.

The specular reflectance measurement apparatus, shown in Fig. 2(a), consists of a Tx part, a Rx part, and an MUT holder located at the center of the Tx and Rx parts, where the Tx and Rx parts consist of a horn antenna and a frequency extender. The Tx and Rx parts and the MUT holder are installed on manual/motorized stages and slides for aligning and fixing them. For adjusting the separation distance between the Tx and Rx
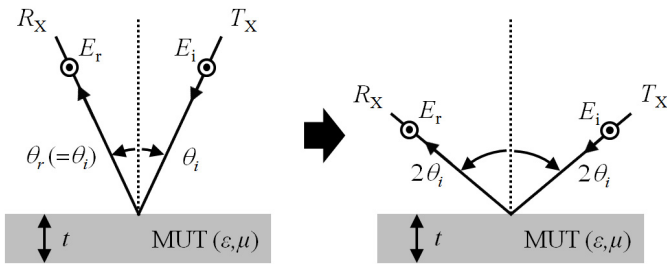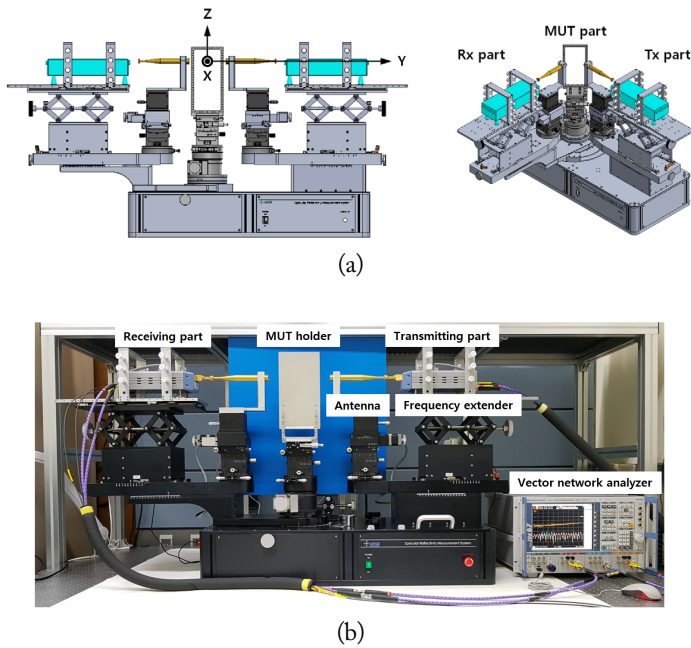

Fig. 1. Conventional specular reflection measurement configuration (MUT is kept fixed, while the Tx part and Rx part, with respect to the surface normal of the MUT, are simultaneously varying with the same speed).

(a)

(b)

Fig. 2. (a) Schematic diagram of the specular reflectance measurement apparatus. (b) Implemented specular reflectance measurement system.
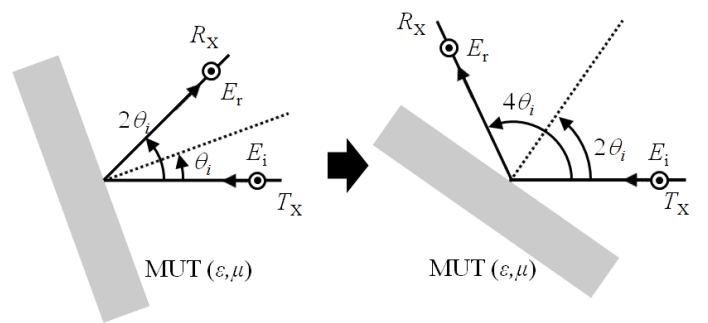

Fig. 3. Proposed specular reflection measurement configuration (The Tx part is kept fixed, while the Rx part and MUT are concentric-rotating with a 2:1 speed ratio).

antennas and the MUT, a manual Y slide is installed below each Tx and Rx part. Table 1 shows the configuration of the stages and slides and their degrees of freedom, where the Y and Z axes in Fig. 2(a) and Table 1 correspond to the line of sight from the MUT toward the Tx antenna and the rotation axis of the MUT holder, respectively.

Usually, during specular reflectance measurements, an MUT is kept fixed, and the angle of the incident wave radiated by the Tx part and that of the reflected wave received by the Rx part, with respect to the surface normal of the MUT, are simultaneously varying with the same speed [16], as depicted in Fig. 1. However, such a specular measurement scheme is not suitable for high frequency ranges, because the Tx and Rx parts, consisting of the horn antenna and frequency extender, are bulky. In this case, it is more efficient if one of the Tx and Rx parts is kept fixed, while the other and the MUT is rotated [17]. Here, the Tx part is kept fixed, while the Rx part and the MUT holder are concentric-rotating with a 2:1 speed ratio for allowing specular reflec-tance measurements, as depicted in Fig. 3, where the rotation angle of the MUT, equal to the angle of the incident wave, is half the rotation angle of the Rx part.

To minimize the edge diffraction effects of an MUT in free-space specular reflectance measurements without using EM absorbers, a Gaussian-beam-forming corrugated horn antenna, with a nominal power gain of 27 dB and an axially symmetrical beam with low side lobes, as given in Table 2, is used as Tx and Rx antennas.

The specular reflectance measurement apparatus is capable of being operated in the incident angle range of 30°–70° from the surface normal of an MUT. The lowest possible angle (30°) is restricted due to the size of the Tx and Rx parts. The highest angle (70°) is ascribed to the MUT size and the Gaussian-beam waste size of the Tx and Rx antennas, as the antenna beam size projected on the surface of an MUT increases with the incident angle.

IV. MEASUREMENT PROCEDURE OF SPECULAR REFLECTANCE

For minimizing the measurement errors inherent in the specular reflectance measurements of an MUT, a measurement procedure may consist of the following steps: 1) alignment of the Tx and Rx antennas and the MUT, 2) measurement of the

Table 1. Configuration of stages and slides and their degrees of freedom

Part name	Detail	Configuration and type of stage and slide		Degree of freedom
		Manual	Motorized	
Tx part	Antenna fixture	Z/X/θ_x/θ_y/rotation stage	Y stage	6
	Frequency extender fixture	θ_{xy}/Z/Y slide	-	3
	Base stage	Y slide	-	1
MUT holder	MUT fixture	X/Y/θ_x/θ_y/rotation stage	Z rotation stage	6
Rx part	Antenna fixture	Z/X/θ_x/θ_y/rotation stage	Y stage	6
	Frequency extender fixture	θ_{xy}/Z/Y slide	-	3
	Base stage	Y slide	Z rotation stage	2

Y and Z axes correspond to the line of sight from the MUT toward the Tx antenna and the rotation axis of the MUT holder, respectively.

Table 2. Specifications of Tx and Rx antennas

Type	Gaussian-beam-forming corrugated horn antenna				
Features	Axially symmetrical beams with low side lobes				
Frequency band	D-band		G-band		J-band
Operating frequency range (GHz)	110–170		140–220		220–325
Aperture diameter (D, mm)	28		23		17
Length (mm)	244		205		137
Waveguide connector	WR-6.5		WR-5.1		WR-3.4
Gain (dB)	27		27		27
Fresnel region $\left(0.62\sqrt{\frac{D^3}{\lambda}} < R < 2\frac{D^2}{\lambda}\right)$	110 GHz	56–575 mm	140 GHz	47–494 mm	220 GHz	37–424 mm
	140 GHz	63–732 mm	170 GHz	51–600 mm	260 GHz	40–501 mm
	170 GHz	69–889 mm	220 GHz	59–776 mm	325 GHz	45–626 mm

D and R are the largest dimension of an antenna aperture and the separation distance from the antenna, respectively.

specular reflection coefficients of the metal plate used as the reflection standard and the MUT, 3) calculation of the specular reflectance of the MUT, and 4) minimization of multiple reflection effects between the Tx and Rx antennas and the MUT on the measured specular reflectances.

1. Alignment of the Tx and Rx Antennas and the MUT

1-1) Rotate the Rx part in the opposite direction of the Tx part with respect to the rotation axis of the MUT holder. Set the rotation angle of the Rx part to 180° under the assumption that the rotation angle of the Tx part is 0°.

1-2) Install a Gaussian-beam-forming corrugated horn antenna and a frequency extender on both the Tx and Rx parts.

1-3) Align the Tx and Rx antennas to make the two antennas face each other with respect to the rotation axis of the MUT holder.

1-4) Vertically install a rectangular metal plate with a good planarity on the MUT holder, and align the center of the plate surface with the rotation axis of the MUT holder.

1-5) Rotate the metal plate to make the plate surface parallel to the line of sight connecting the two antennas. Set the rotational angle of the MUT holder to 90°.

1-6) Adjust the separation distance between the respective apertures of the Tx and Rx antennas and the rotation axis of the MUT holder to be the same.

1-7) Before connecting the antenna to the frequency extender at both the Tx and Rx parts, perform a one-port calibration at the test port of the Tx and Rx frequency extenders under the measurement conditions of 100 MHz frequency step and 100 Hz IF bandwidth over an operating frequency range of the frequency extender. Connect the antenna to the test port of the calibrated frequency extender at both Tx and Rx parts.

1-8) Rotate the MUT holder to the rotation angle of 0° to make the metal plate surface and the Tx antenna face each other.

1-9) Search the rotation angle of the MUT holder where the magnitude of the reflection coefficient (S_{11}^{Tx}) of the metal plate at the Tx part is the maximum in the vicinity of 0°. Set the rotation angle of the MUT holder to 0°.

1-10) Rotate the MUT holder to the rotation angle of 180° to make the surface of the metal plate and the Rx antenna face each other.

1-11) Search the rotation angle of the Rx part where the magnitude of the reflection coefficient (S_{22}^{Rx}) of the metal plate at the Rx part is the maximum in the vicinity of 180°. Set the rotation angle of the Rx part to 180°.

2. Measurement of the Specular Reflection Coefficients of the Metal Plate and the MUT

2-1) Measure the forward and backward directional transmission coefficients (S_{21}^{metal} and S_{12}^{metal}) between the Tx and Rx antennas, which correspond to each directional specular reflection coefficient of the metal plate (theoretically assumed to be −1) in the incident angle range of 30°–70° with a 0.5° step by using the S-parameter measuring instrument. The incident angle in the 30°–70° range corresponds to the rotation angle of the MUT holder in the 30°–70° range and that of the Rx part in the 60°–140° range.

2-2) Rotate the MUT holder and Rx part to the rotation angle of 90° and 180°, respectively.

2-3) Replace the metal plate with an MUT (a rectangular dielectric plate under test). If the thickness of the MUT is different from that of the metal plate, align the center of the MUT surface with the rotation axis of the MUT holder.

2-4) Measure the forward and backward directional transmission coefficients (S_{21}^{MUT} and S_{12}^{MUT}) between the Tx and Rx antennas, which correspond to each directional specular reflection coefficient of the MUT in the incident angle range of 30°–70° with a 0.5° step by using the S-parameter measuring instrument.

3. Calculation of the Specular Reflectance of the MUT

3-1) Calculate the forward and backward directional specular reflectance of an MUT, which is defined by the specular re-

flection power of an MUT normalized to that of the metal plate at each direction, i.e., $\left|S_{21}^{\mathrm{MUT}}/S_{21}^{\mathrm{metal}}\right|^2$ and $\left|S_{12}^{\mathrm{MUT}}/S_{12}^{\mathrm{metal}}\right|^2$.

3-2) Calculate the specular reflectance (SR_{Specular}) of an MUT, which is defined by the average of the forward and backward directional specular reflectance of an MUT:

$$SR_{\mathrm{Specular}} = \frac{\left|S_{21}^{\mathrm{MUT}}/S_{21}^{\mathrm{metal}}\right|^2 + \left|S_{12}^{\mathrm{MUT}}/S_{12}^{\mathrm{metal}}\right|^2}{2}. \qquad (3)$$

3-3) Repeat four times the specular reflectance measurement, changing the separation distances between the Tx and Rx antennas by $\lambda/8$ intervals (i.e., $d = d_0 + n\lambda/8$, $n = 0, 1, 2, 3$, where d, d_0, and λ are the separation distance, the initial separation distance, and the wavelength of the signal, respectively).

4. Minimization of Multiple Reflection Effects between the Tx and Rx Antennas and the MUT on the Measured Specular Reflectances

4-1) Multiple reflection effects between the Tx and Rx antennas and the MUT can be minimized by averaging out the four measured specular reflectances as follows:

$$SR_{\mathrm{Specular}}^{\mathrm{Average}} = \frac{1}{4}\sum_{n=0}^{3} SR_{\mathrm{Specular}}\left(d = d_0 + \frac{n\lambda}{8}\right). \qquad (4)$$

V. MEASUREMENT RESULTS

Perpendicular-polarized specular reflectances of commonly used dielectric plates with a rectangular shape, as shown in Table 3, are measured by using the proposed specular reflectance measurement system in the incident angle of 30°–70° at nine frequencies that are equally selected from the three waveguide frequency bands. The selected nine measurement frequencies are 110 GHz, 140 GHz, and 170 GHz from the D-band; 140 GHz, 170 GHz, and 220 GHz from the G-band; and 220

GHz, 260 GHz, and 325 GHz from the J-band, where 140–170 GHz is the overlapped frequency range of the D-/G-bands, and 220 GHz is the boundary frequency of the G-/J-bands.

In the specular reflectance measurements, the separation distance between the respective apertures of the Tx and Rx antennas and the surface of an MUT and a metal plate is 110 mm in the D-/G-bands and 127 mm in the J-band, respectively, which means that these reflectance measurements are performed in the Fresnel (or radiating near-field) region of each antenna as shown in Table 2. The Fresnel region is defined by $0.62\sqrt{\frac{D^3}{\lambda}} < R < 2\frac{D^2}{\lambda}$, where D and R are the largest dimension of an antenna aperture and the separation distance from the antenna, respectively [18].

For a rectangular acetal plate of 2.030 mm thickness and a 20 cm × 35 cm size, four specular reflectances, which were measured with changing the separation distance between the Tx and Rx antennas by $\lambda/8$ intervals, their averaged-out reflectance, and the analytic reflectance are shown at 140 GHz of the G-band and 220 GHz of the J-band as depicted in Fig. 4(a) and (b), respectively. Fig. 4 shows at the two frequencies that (1) multiple reflection effects between the Tx and Rx antennas and the MUT on the measured specular reflectances can be minimized by averaging out the multiple specular reflectances measured at the different separation distances by $\lambda/8$ intervals, and (2) the measured specular reflectances can be verified by the fact that the averaged-out results (green line with dot) and the theoretical ones (black dot) agree well with each other. This means that the specular reflectance measurement system can be effectively calibrated to minimize the measurement errors inherent in the measurement system in the Fresnel region of Tx and Rx antennas. The theoretical specular reflectances are calculated by using (1) and (2) above with the complex relative permittivity of acetal with 2.030 mm thickness, in this case $\varepsilon_r = 2.800 - j0.043$, which is measured by using a quasi-optic free-space material measurement system [8, 9].

Measured specular reflectances of commonly used dielectric plates, as listed in Table 3, are shown in Figs. 5–14, whose upper,

Table 3. MUT name, its dimension, and the figure number of its measured specular reflectance

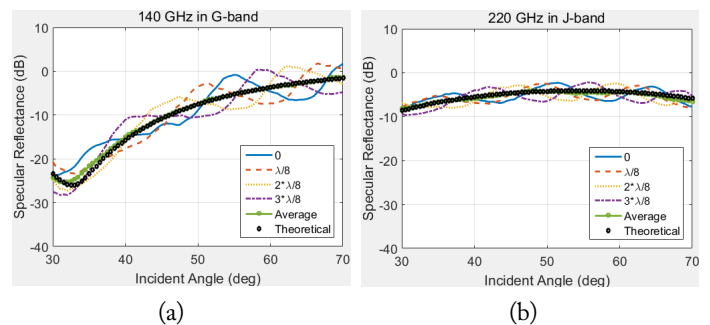| MUT	Dimension		Figure number
	Thickness (mm)	Width × Height (cm²)	
Acetal	2.030, 5.644	20 × 35	5, 6
Acryl	2.010, 5.055	20 × 35	7, 8
Bakelite	2.210, 5.163	20 × 35	9, 10
PC (polycarbonate)	2.010, 4.955	20 × 35	11, 12
PVC (polyvinyl chloride)	1.730, 5.138	20 × 35	13, 14

Fig. 4. Specular reflectance of an acetal plate of 2.030 mm thickness. (a) 140 GHz of the G-band. (b) 220 GHz of the J-band.

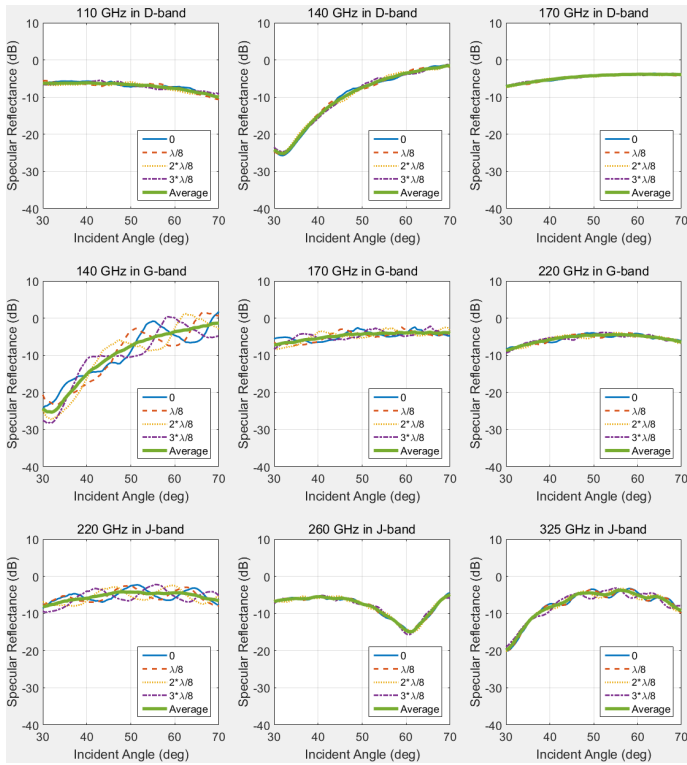Fig. 5. Specular reflectance of an acetal plate of 2.030 mm thickness.

Fig. 7. Specular reflectance of an acryl plate of 2.010 mm thickness.

middle, and lower correspond to the specular reflectances measured in the D-/G-/J-bands, respectively. Regardless of the kind of MUTs, Figs. 5–14 show, in the Fresnel region of Tx and Rx antennas, that 1) multiple reflection effects between the two
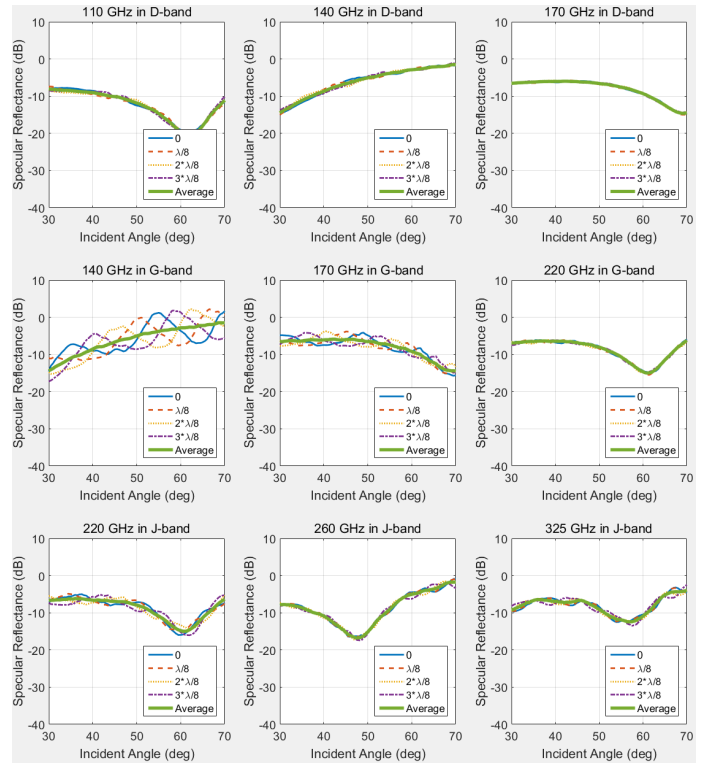
antennas and the MUT can be minimized by averaging out the multiple specular reflectances measured at the different separation distances by λ/8 intervals, 2) the multiple reflection effects in the D-band are weaker than in the G-/J-bands, and 3) the
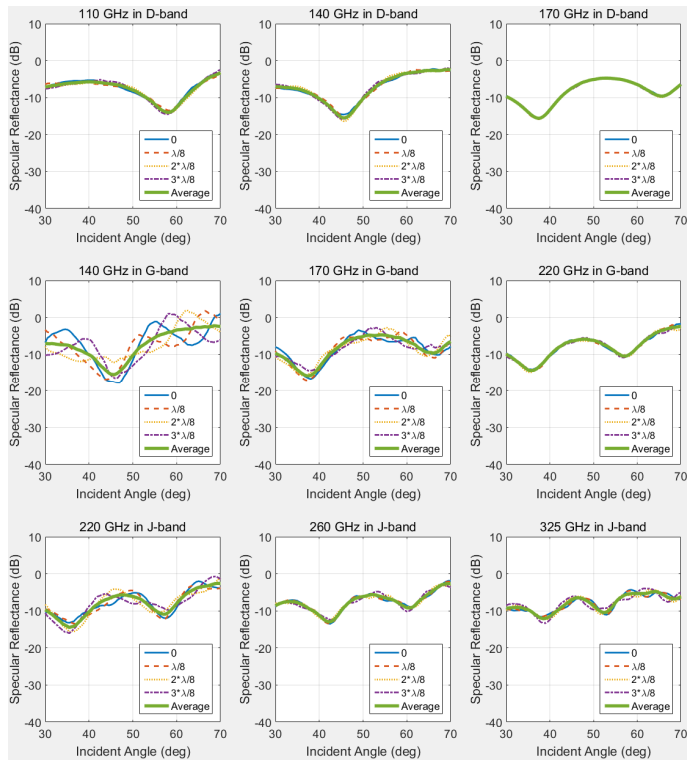

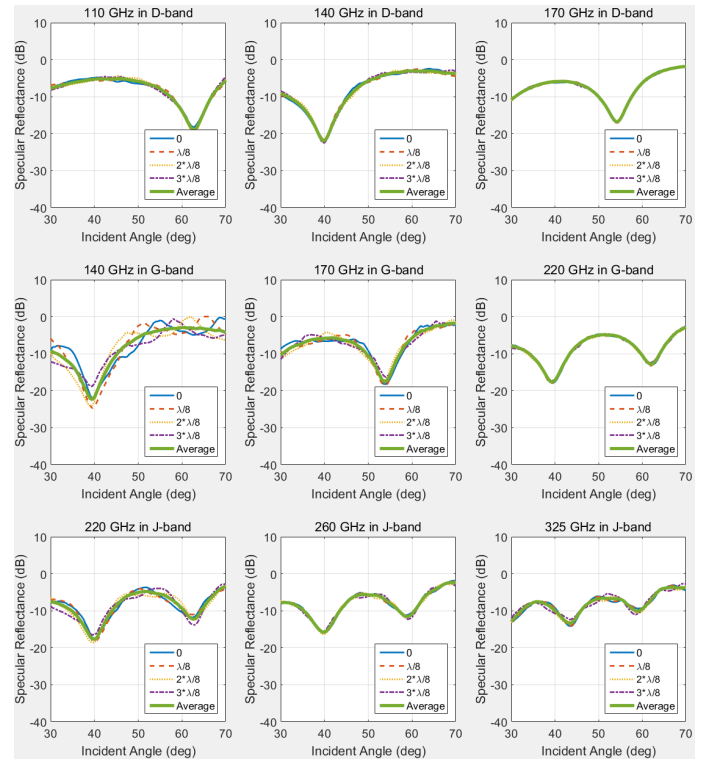Fig. 6. Specular reflectance of an acetal plate of 5.644 mm thickness.

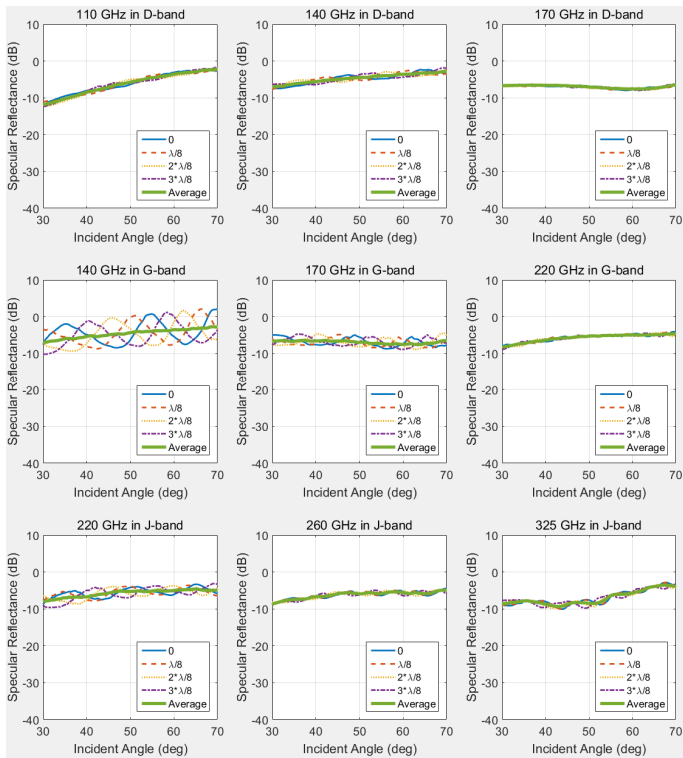Fig. 8. Specular reflectance of an acryl plate of 5.055 mm thickness.

Fig. 9. Specular reflectance of a bakelite plate of 2.210 mm thickness.

Fig. 11. Specular reflectance of a PC plate of 2.010 mm thickness.

measured specular reflectances can be verified by the fact that the measured results over the two overlapped frequencies of the D-/G-band, i.e., 140 GHz (the center of the upper and the left of the middle in Figs. 5–14) and 170 GHz (the right of the up-
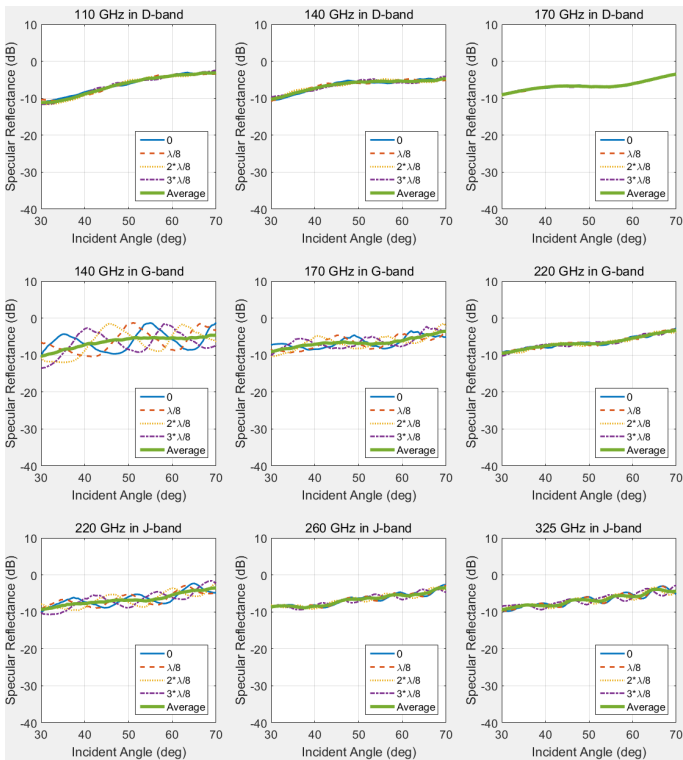
per and the center of the middle), and at the boundary frequency of the G-/J-band, i.e., 220 GHz (the right of the middle and the left of the lower), agree well with the results for the other band, respectively.

Fig. 10. Specular reflectance of a bakelite plate of 5.163 mm thickness.
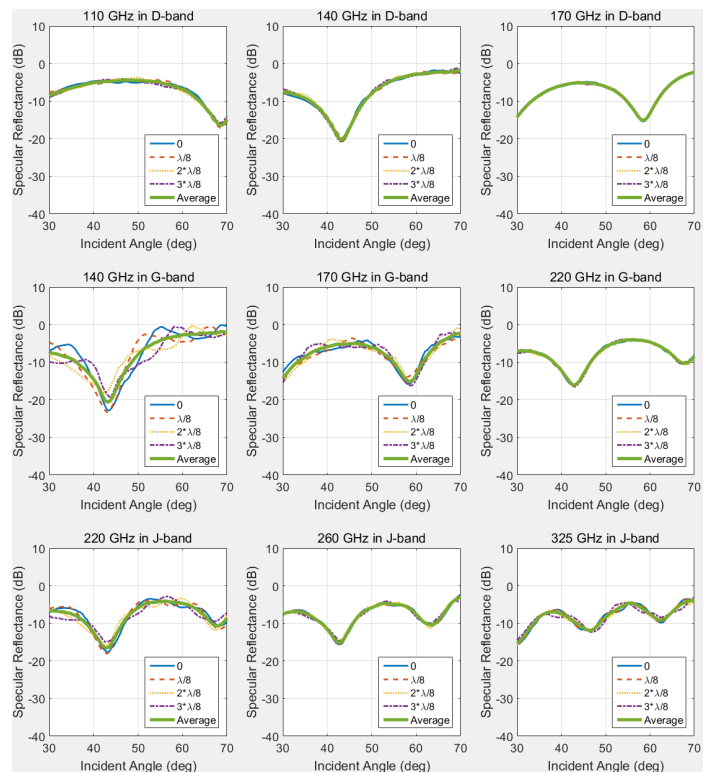

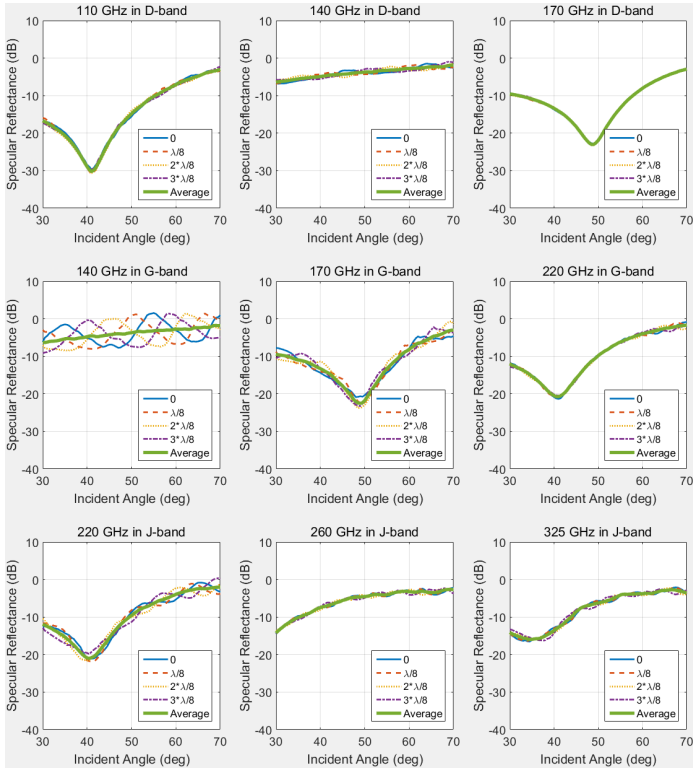Fig. 12. Specular reflectance of a PC plate of 4.955 mm thickness.

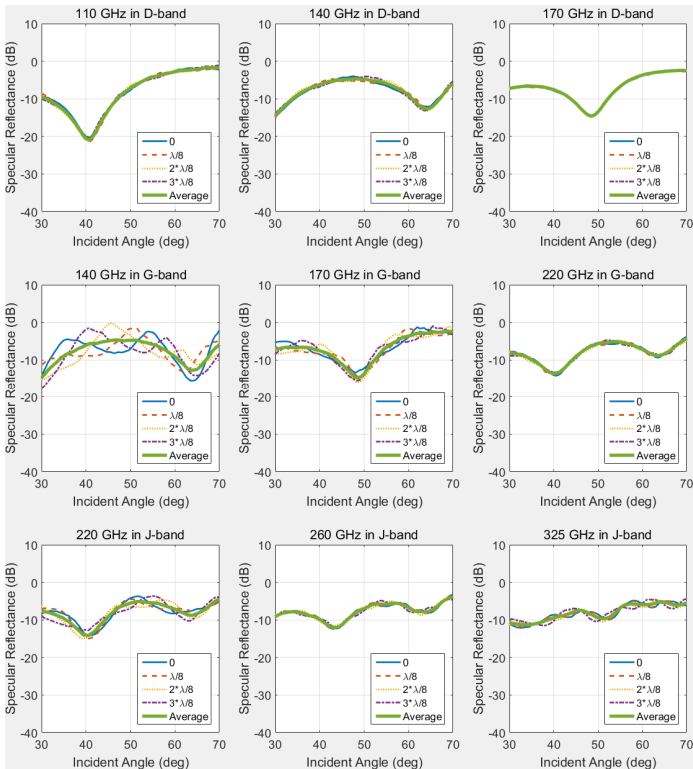Fig. 13. Specular reflectance of a PVC plate of 1.730 mm thickness.

Fig. 14. Specular reflectance of a PVC plate of 5.138 mm thickness.

VI. Concluding Remarks

In this paper, specular reflectance measurements of dielectric plates are described in the 110–325 GHz frequency range, i.e.,

three waveguide frequency bands: D-band (110–170 GHz), G-band (140–220 GHz), and J-band (220–325 GHz).

The proposed specular reflectance measurement system consists of an *S*-parameter measuring instrument and a specular reflectance measurement apparatus. The Tx part of the specular reflectance measurement apparatus is kept fixed, while the Rx part and the MUT holder are concentric-rotating with a 2:1 speed ratio for allowing specular reflectance measurements.

The specular reflectance measurement system is effectively calibrated to minimize the measurement errors inherent in the measurement system in the following ways: 1) by using a Gaussian-beam-forming corrugated horn antenna with an axially symmetrical beam with low side lobes to minimize the edge diffraction effects of an MUT in free-space measurements without using EM absorbers, 2) by normalizing the specular reflection power of an MUT to that of a metal plate used as the reflection standard, and 3) by averaging out the multiple specular reflectances measured with changing the separation distance between the Tx and Rx antennas by $\lambda/8$ intervals to minimize the multiple reflection effects between the two antennas and an MUT on the measured specular reflectances.

Measurement results of the perpendicular-polarized specular reflectance of commonly used dielectric plates are verified in the Fresnel region of Tx and Rx antennas by the fact that 1), for acetal, the average of the multiple specular reflectances measured with changing the separation distance between the Tx and Rx antennas by $\lambda/8$ intervals agrees well with the analytic result, and 2) the results measured at the two overlapped frequencies of the D-/G-bands, i.e., 140 GHz and 170 GHz, and at the boundary frequency of the G-/J-bands, i.e., 220 GHz, agree well with the results at the other band for all of MUTs, respectively.

References

[1] T. M. Nguyen and J. Y. Chung, "RF conductivity measurement of conductive Zell fabric," *Journal of Electromagnetic Engineering and Science*, vol. 16, no. 1, pp. 24–28, 2016.

[2] G. Y. Kim and B. S. Lee, "Synthesis of bulk medium with negative permeability using ring resonators," *Journal of Electromagnetic Engineering and Science*, vol. 16, no. 2, pp. 67–73, 2016.

[3] B. Komiyama, M. Kiyokawa, and T. Matsui, "Open resonator for precision dielectric measurements in the 100 GHz band," *IEEE Transactions on Microwave Theory and Techniques*, vol. 39, no. 10, pp. 1792–1796, 1991.

[4] S. N. Dudorov, D. V. Lioubtchenko, J. A. Mallat, and A. V. Raisanen, "Differential open resonator method for permittivity measurements of thin dielectric film on substrate," *IEEE Transactions on Instrumentation and Measurement*, vol. 54, no. 5, pp. 1916–1920, 2005.

[5] D. K. Ghodgaonkar, V. V. Varadan, and V. K. Varadan, "Free-space measurement of complex permittivity and complex permeability of magnetic materials at microwave frequencies," *IEEE Transactions on Instrumentation and Measurement*, vol. 39, no. 2, pp. 387–394, 1990.

[6] D. Bourreau, A. Peden, and S. Le Maguer, "A quasi-optical free-space measurement setup without time-domain gating for material characterization in the W-band," *IEEE Transactions on Instrumentation and Measurement*, vol. 55, no. 6, pp. 2022–2028, 2006.

[7] A. Kazemipour, M. Hudlicka, S. K. Yee, M. A. Salhi, D. Allal, T. Kleine-Ostmann, and T. Schrader, "Design and calibration of a compact quasi-optical system for material characterization in millimeter/submillimeter wave domain," *IEEE Transactions on Instrumentation and Measurement*, vol. 64, no. 6, pp. 1438–1445, 2015.

[8] J. S. Kang, J. H. Kim, C. H. Cho, and D. C. Kim, "W-band permittivity measurements using a free-space material measurement technique," *The Journal of Korean Institute of Electromagnetic Engineering and Science*, vol. 24, no. 3, pp. 253–258, 2013.

[9] J. S. Kang, J. H. Kim, and J. I. Park, "Reduction of edge diffraction effects of MUT holder using EM absorber in W-band free-space material measurements," in *Proceedings of the 2016 International Symposium on Antennas and Propagation (ISAP)*, Okinawa, Japan, 2016, pp. 936–937.

[10] S. Iyer, C. C. Cheng, C. Kim, and A. Abbaspour-Tamijani, "Compact Gaussian beam system for S-parameter characterization of planar structures at millimeter-wave frequencies," *IEEE Transactions on Antennas and Propagation*, vol. 59, no. 9, pp. 2437–2444, 2010.

[11] F. Sagnard, F. Bentabet, and C. Vignat, "*In situ* measurements of the complex permittivity of materials using reflection ellipsometry in the microwave band: theory (Part I),"

[12] F. Sagnard, F. Bentabet, and C. Vignat, "*In situ* measurements of the complex permittivity of materials using reflection ellipsometry in the microwave band: theory (Part II)," *IEEE Transactions on Instrumentation and Measurement*, vol. 54, no. 3, pp. 1274–1282, 2005.

[13] M. Klenner, C. Zech, A. Hulsmann, J. Kuhn, M. Schlechtweg, and O. Ambacher, "Spectroscopic measurement of material properties using an improved millimeter-wave ellipsometer based on metallic substrates," *IEEE Transactions on Instrumentation and Measurement*, vol. 65, no. 11, pp. 2551–2559, 2016.

[14] IEEE 802.15 WPAN Terahertz Interest Group (IGthz) [Online]. Available: http://www.ieee802.org/15/pub/IGthz-OLD.html.

[15] J. S. Kang, J. H. Kim, K. Y. Kang, D. H. Yoon, and S. W. Park, "Specular reflectance measurement of dielectric plates in 110–325 GHz frequency range," in *Proceedings of the 39th Annual Meeting and Symposium of the Antenna Measurement Techniques Association (AMTA)*, Atlanta, GA, 2017.

[16] M. H. Umari, D. K. Ghodgaonkar, V. V. Varadan, and V. K. Varadan, "A free-space bistatic calibration technique for the measurement of parallel and perpendicular reflection coefficients of planar samples," *IEEE Transactions on Instrumentation and Measurement*, vol. 40, no. 1, pp. 19–24, 1991.

[17] X. Faget, N. Mallejac, and A. Litman, "Bistatic free-space measurements of magneto-dielectric materials and comparison with numerical models," in *Proceedings of the 2016 URSI International Symposium on Electromagnetic Theory (EMTS)*, Espoo, Finland, 2016, pp. 404–406.

[18] C. A. Balanis, *Modern Antenna Handbook*. New York, NY: John Wiley & Sons, 2008.

Jin-Seob Kang

received the B.S. degree in electronic engineering from Hanyang University, Seoul, Korea, in 1987, and the M.S. and Ph.D. degrees in electrical engineering from Korea Advanced Institute of Science and Technology (KAIST), Daejeon, Korea, in 1989 and 1994, respectively. He was a Postdoctoral Research Associate with the Department of Electrical and Computer Engineering, University of Illinois at Urbana-Champaign, in 1995 and an Assistant Professor with the School of Electrical and Electronic Engineering, Chungbuk National University, Korea, from 1996 to 1997. He joined the Korea Research Institute of Standards and Science, Daejeon, in 1998. His research interests include electromagnetics measurement standards (scattering parameters, antenna characteristics, field strength, material parameters) and (sub-)mm-wave measurements.

Jeong-Hwan Kim

was born in Cheongju, Korea in 1954. He received the B.S. degree in electrical engineering from Seoul National University, Seoul, Korea in 1978, and the M.S. and the Ph.D. degrees from Korea Advanced Institute of Science and Technology, Seoul, Korea in 1980 and 2000, respectively, both in electrical and electronic engineering. He joined the Center for Electromagnetic Wave, the Korea Research Institute of Standards and Science, Daedeok Science Town, Korea in 1981. Since then, he has been working on the developments of the six-port ANA systems, standard antennas, and electromagnetics measurement standards.

Kwang-Yong Kang

was born in Sacheon, Korea in 1951. He received the B.S. degree from Seoul National University, Seoul, Korea, in 1975, and the Ph.D. degree in solid-state physics from Pusan National University, Busan, Korea, in 1988. Since 1989, he has been a member of engineering staff of the ETRI, Daejeon, Korea. He was a member of the IEEE MTT and OSA of USA, JJAP of Japan, and KEES/KPS of Korea. He retired from the institute (ETRI), passed through the university, and he is working for a research institute of a small company, Panoptics Corp. He is now continuing his research work (THz field) at the Lab. of the Corporate Research Lab. His research interests include the HTS thin films and millimeter-wave device, metal-insulator transition (MIT) devices, and terahertz technologies.

Sung Won Park

received the M.S. degree in information and communications engineering from Kyunghee University, Seoul, Korea, in 2003. He joined the National Radio Research Agency, Naju, Korea, in 2003 and in 2013, he was promoted to Deputy Director.

Dae-Hwan Yoon

received the B.S. degree in electronic engineering from Chosun University, Gwangju, Korea, in 2007. He joined the Gwangju Radio Management Service, Naju, Korea, from 2008 to 2014. He joined the National Radio Research Agency, Naju, Korea, in 2015.